Piattoni, Q., Freddi, F., Zona, A., Leoni, G., Dall'Asta, A, Argentoni, A. (2020) Seismic Design of Innovative Steel Frames with Partially-Prefabricated Infill Walls. The 9th European Conference on Steel and Composite Structures (Eurosteel 2020), Sheffield, UK, 1–3 September 2021. https://doi.org/10.1002/cepa.1501

Seismic design of innovative steel frames with partially-prefabricated infill walls

Quintilio Piattoni [1], Fabio Freddi [2], Alessandro Zona [1], Graziano Leoni [1], Andrea Dall'Asta [1], Alessio Argentoni [3]

Correspondence

Prof. Alessandro Zona
University of Camerino,
School of Architecture and Design,
Viale della Rimembranza 3,
Ascoli Piceno, 63100 Italy
Email: alessandro.zona@unicam.it

Abstract

Hybrid steel and concrete seismic-resistant systems made by steel frames with reinforced concrete infill walls (SRCWs) have potential advantages over structural solutions made only by steel or reinforced concrete (RC). In fact, the high initial stiffness of concrete is useful to minimize the damage of non-structural elements under frequent (low to moderate) earthquakes while the ductility and dissipative capacity of the steel allow good performances under rare (high-intensity) events. Eurocode 8 considers SRCW systems to behave essentially as RC walls. However, numerical analyses on SRCWs, designed according to the Eurocodes, pointed out an unsatisfactory seismic behaviour with discrepancies between the behaviour assumed in the design and the simulated response under seismic actions. Indeed, the idea of stiffening a steel frame with a RC infill leads complex mechanisms that are difficult to control as being affected by many variables. In this study, some of the recent developments made for innovative SRCW are transferred to hybrid steel and concrete walls with partially-prefabricated infills. Numerical models are analysed to understand the global behaviour of the considered SRCWs and to provide a preliminary validation of the proposed structural solution.

Keywords

Finite element models, Nonlinear analysis, Seismic design, Steel-concrete hybrid structures.

1 Introduction

Reinforced concrete (RC) walls are employed as structural systems resisting horizontal loads to increase both the lateral stiffness and strength of buildings [1]. Accordingly, the use of RC walls allows the reduction of the seismic damage of the non-structural elements and to resist the induced seismic shear forces. Seismic design recommendations for RC walls are detailed in many building codes, including Eurocode 8 [2]. However, RC walls are difficult to repair when struck by seismic events that exceed their elastic threshold. Hybrid steel and reinforced concrete walls provide a possible alternative to conventional RC walls as seismic-resisting systems. If properly conceived and designed, hybrid walls combine the benefits of RC walls (stiffness) and steel elements (ductility, energy dissipation, possibility to replace damaged parts). The review of the state of the art, e.g. [3], shows that many studies focused on the seismic performances of hybrid coupled walls (HCW) and of steel frames with RC infill walls (SRCW). However, seismic design provisions are generally very limited, e.g. few indications provided in Eurocode 8 [2].

HCW systems can be obtained coupling two RC walls [4] or one RC wall to two side steel columns [5] by means of steel coupling links. The latter configuration of HCW is a recent proposal, still under investigation, e.g. [6-8], for a number of improvements and validation requiring further studies, including the possible use of dampers or fuses in the steel coupling links, e.g. [9].

SRCW systems include different typologies, e.g. RC walls with encased steel profiles [10], RC walls with steel plates enhanced with concrete-filled steel tubes [11], prefabricated concrete-filled steel tubular framework composite slabs [12], RC walls with steel plates [13], use innovative materials in order to strengthen the RC infill walls of the hybrid systems [14], [15] and steel frames with RC infill walls [3], [16].

The present study focuses on the development of SRCWs starting from the solution proposed in [3], [16], i.e. steel frames with RC infill walls conceived as a statically determinate structural scheme where the RC infill walls work as diagonal struts while energy dissipation occurs in the vertical steel elements yielding in tension. A tailored capacity design procedure was developed consistently with the Eurocode framework for seismic design. Preliminary numerical and experimental studies [3], [16] together with the evaluation of constructive aspects and economic competitiveness [3] as compared to conventional bracing systems adopted in steel structures, opened the way to the potential use of the developed SRCWs in real world engineering applications. However, this hy-

1. University of Camerino, School of Architecture and Design, Ascoli Piceno, Italy.
2. University College of London, Department of Civil, Environmental and Geomatic Engineering, London, UK.
3. Tecnostrutture s.r.l., Noventa di Piave, Venice, Italy.

brid structural system needs supplementary investigations to provide more insight into structural behaviour, e.g. influence of shear connection distributions [17], as well as more insights and possible optimization of constructional/technological aspects, e.g. replacement of the dissipative steel elements.

Starting from the obtained results, a novel SRCWs system was developed [18] with the support of Tecnostrutture s.r.l. (Noventa di Piave, Italy), leader in the light and heavy concrete prefabricated construction sector for over 30 years, including a varied range of steel and concrete prefabricated systems widely used in civil and industrial engineering projects. The main objective that the SRCW was expected to meet was the limitation of the damages of the non-structural elements under low-to-moderate earthquakes which is a crucial aspect in seismic design, particularly for steel structures, e.g. [19], [20]. To this end the design of the proposed SRCW was based on the hypothesis that the hybrid shear walls remain in the elastic range when design seismic events occur. This assumption allows overcoming the lack of design rules in the Eurocode 8 [2] for these systems. Preliminary analyses were presented in [18] to evaluate the seismic performances of this elastic SRCW. In the present paper such aspect is further investigated through the analysis of the seismic behaviour of SRCWs connected to moment-resisting (MR) steel-concrete composite frames, thus, in a dual wall-MR scheme that faces horizontal actions.

2 Structural concept of the proposed SRCWs

The considered SRCWs have columns with concrete-filled hollow section and horizontal beams with wide-flange cross section beams (Figure 1). There are stiffened plates at each corner of the hybrid wall (Figures 1 and 2).

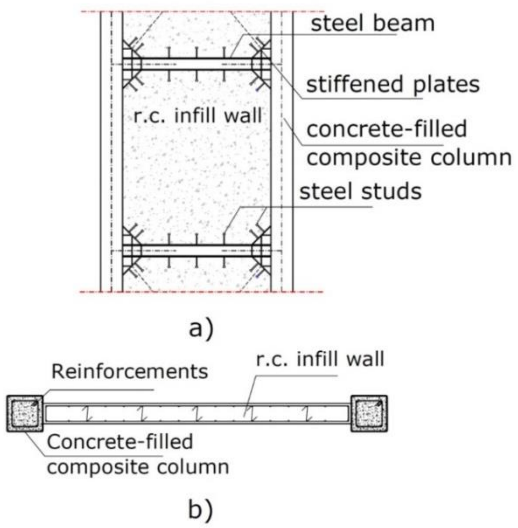

Figure 1 SRCW system with concrete-filled hollow section columns: frontal view (a) and horizontal section (b).

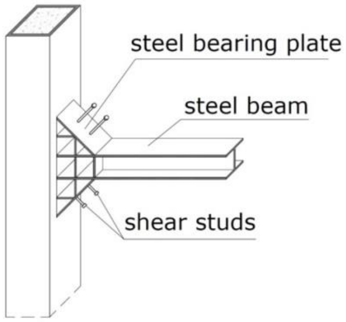

Figure 2 Corner of a SRCW system.

The concrete-filled hollow section columns were preferred to other solutions in order to more conveniently allow the connection between the SRCWs and the MR frames. In fact, MR frames in the present study were considered having columns with concrete-filled hollow section columns and composite truss beams with a bottom steel plate (Figure 3), partially precast and completed in situ by concrete casting, a solution developed by Tecnostrutture.

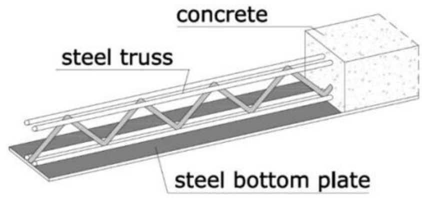

Figure 3 Steel-concrete composite truss beam.

The hybrid wall has shear studs at the corners and along the horizontal steel beams (Figure 1). The steel studs bear the shear forces between the RC wall and the frame of the hybrid system. In addition, the shear studs oppose to the out-of-plane overturning of the RC infill wall and increment the stiffness of the SRCW. The considered hybrid systems do not have steel studs along the vertical columns, as in the solution developed and tested in [3], [16]. The thickness of the infill RC wall is equal to the width of the flange of the horizontal beams of the SRCWs.

Diagonal struts with compressive axial forces, are formed within the frame when horizontal forces are applied to the SRCW system. The stiffened plates at the corner of the hybrid system facilitate the formation of these inclined struts along the diagonals of the RC infill walls as shown in Figure 4.

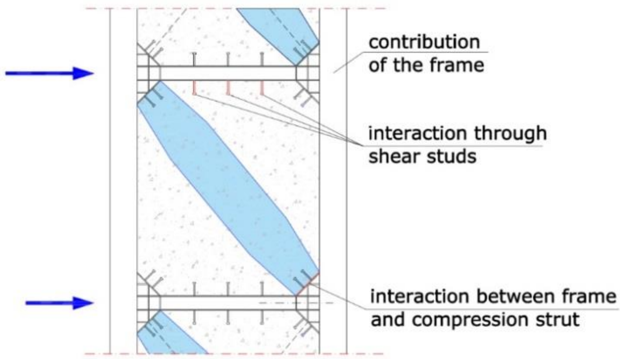

Figure 4 Resisting-mechanisms to horizontal actions for a SRCW system.

Given that the SRCWs proposed in this study have continuous columns, beam-to-column joints stiffened with the inclined plates, and are connected to the composite truss beams of the MR hybrid frames, a statically redundant scheme (Figure 5) is preferred over the truss-like statically-determinate structures used in [3], [16]. Accordingly, the concrete-filled composite columns of the SRCWs are affected by both axial force and bending moments.

Three horizontal resisting mechanisms can be identified: (1) contribution of the MR frame made of concrete-filled composite columns and steel beams; (2) contribution of the diagonal struts formed in the RC infill walls; (3) resisting mechanism due to the interactions between the steel-concrete composite frame and the RC infill wall through friction and shear connectors.

The assumption of this study that SRCWs are designed to remain in their elastic range when the design seismic events occur, leads to the behaviour factor equal to 1.5 according to both Eurocode 8 [2] and the Italian building code [21]. Thus, capacity design rules and the need of certifications or technical approvals for the innovative structural solution are avoided.

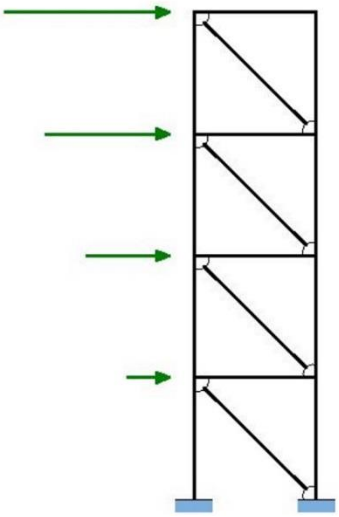

Figure 5 Structural representation for a SRCW system.

3 Design and verification rules for the proposed SRCWs

3.1 General framework

The adopted design and verification rules, hereafter described in details, are derived from indications available in Eurocodes 2, 3, 4, and 5 [2], [22-24], for similar resisting mechanisms. In this way, the presented formulation could be considered consistent with the framework of the Eurocodes.

3.2 Inclined steel bearing plates

The inclined steel bearing plates (previously introduced in Figure 1 and 2) are added to the beam-to-column node to facilitate the formation of diagonal struts within the RC infill wall when horizontal forces are applied to the SRCW. The compressive strength of a diagonal strut (Figure 6) is assessed according to the following formula:

$$R_d = \min\left\{0.85\frac{f_{ck}}{\gamma_C}t_w l_b\ ;\ 0.85\frac{f_{ck}}{\gamma_C}\nu\left(1-\frac{f_{ck}}{250}\right)(\alpha t_w l_b)\right\} \tag{1}$$

derived from § 6.5 of Eurocode 2 [22], where f_{ck} is the characteristic compressive cylinder strength of concrete, γ_G is the partial factor for concrete, t_w is the thickness of the infill wall, l_b is the in-plane width of the bearing plate at the diagonal ends whereas the effective width of the diagonal strut is obtained multiplying l_b by a coefficient α > 1 at mid diagonal [16]. This coefficient is calculated according to § 6.5 of Eurocode 2 [22] with the limitation $\alpha \le h/(2l_b)$, being h equal to the length of the diagonal strut. Accordingly, the second formula of the left term of Eq. (1), represents the compressive strength at mid-strut and ν is a coefficient that takes in account the influence of transverse tension (ν may be assumed equal to 0.60 as suggested by Eurocode 2 [22]).

3.3 Reinforcements of the infill wall

The reinforcing bars of the RC infill wall are designed taking in account a tensile force *T* evaluated by the following formula:

$$T = \frac{1}{4}\left(1-\frac{1}{\alpha}\right)N_{Ed} \tag{2}$$

where N_{Ed} is the axial force in the vertical steel elements, thus, combining the effects of the gravity loads with those of the seismic action. Two different reinforcement layouts may be adopted (Figure 6): the first reinforcement layout is characterized by orthogonal steel bars (Figure 6a) and it is simpler but possibly less stiff than the second one with specific transverse reinforcements (Figure 6b). The second layout requires a third layer of reinforcements and hence, it can be used only in the case of sufficiently thick walls.

In the first layout, vertical and horizontal reinforcements should fulfil the following conditions:

$$\frac{T^2}{f_{yd}^2} = A_{sl}^{v2} + A_{sl}^{h2} \tag{3}$$

$$\frac{A_{sl}^h}{A_{sl}^v} = \frac{L}{H} \tag{4}$$

where f_{yd} is the design tensile strength of reinforcing bars, A_{sl}^v and A_{sl}^h are the reinforcing bars along the vertical and horizontal direction, respectively; *L* and *H* are the inter-axis spacing between the columns and the beams of the hybrid shear wall, respectively.

In the second layout, the reinforcing stirrups of the diagonal struts can be determined according to the simple formula:

$$A_s = \frac{T}{f_{yd}} \tag{5}$$

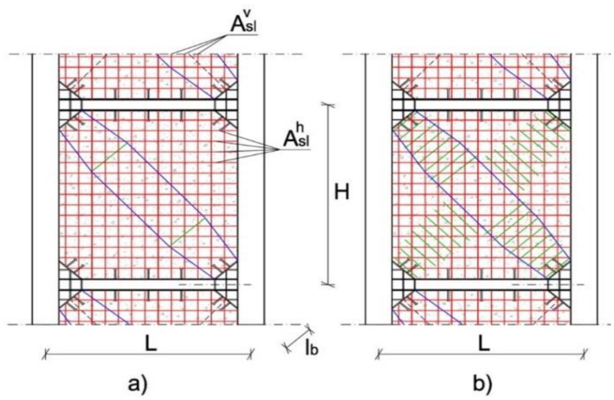

Figure 6 Types of reinforcement: horizontal and vertical steel bars (a) and additional stirrups (b).

3.4 Concrete-filled composite columns

More in details, the verification of the concrete-filled composite columns is carried out according to § 6.7.3 and § 6.7.3.5 of Eurocode 4 [22]. The simplified design method according to §6.7.3.1 of Eurocode 4 [22] is limited to members of doubly symmetrical and uniform cross-section over the member length with rolled, cold-formed, or welded steel sections. The relative slenderness $\bar{\lambda}$ defined in § 6.7.3.3 of Eurocode 4 [22] fulfils the following condition:

$$\bar{\lambda} \le 2 \tag{6}$$

The plastic resistance to compression $N_{pl,Rd}$ of a composite cross-section is calculated by adding the plastic resistances of its components according to following equation of Eurocode 4 (§ 6.7.3.2) [24]:

$$N_{pl,Rd} = A_a f_{yd} + 0{,}85 A_c f_{cd} + A_s f_{sd} \tag{7}$$

where A_a is the cross-sectional area of the structural steel section, A_c is the cross-sectional area of the concrete, A_s is the cross-sectional area of the longitudinal reinforcing bars, f_{yd} is the design value of the yield strength of structural steel, f_{cd} is the design value of the cylinder compressive strength of concrete and f_{sd} is the design value of the yield strength of the reinforced steel. For concrete filled sections the coefficient 0.85 may be replaced by 1.0. Furthermore, the design value of the normal force N_{Ed} should satisfy:

$$\frac{N_{Ed}}{\chi N_{pl,Rd}} \leq 1 \tag{8}$$

where $N_{pl,Rd}$ is the plastic resistance of the composite section according to Equation (7) and to Eurocode 4 [24], but with f_{yd} determined using the partial factor γ_{M1} of Eurocode 3 [23]; χ is the reduction factor for the relevant buckling mode given in §6.3.1.2 of Eurocode 3 [23]. The relative slenderness $\bar{\lambda}$ is given by the following formula:

$$\bar{\lambda} = \sqrt{\frac{N_{pl,Rk}}{N_{cr}}} \tag{9}$$

where $N_{pl,Rk}$ is the characteristic value of the plastic resistance to compression where the characteristic values of the material strengths are used in Equation (7); N_{cr} is the elastic critical normal force for the relevant buckling mode that can be determined as:

$$N_{cr} = \pi^2 \frac{(EI)_{eff}}{l_0^2} \tag{10}$$

where the characteristic value of the effective flexural stiffness $(EI)_{eff}$ of a cross section of a composite column should be calculated by the following equation:

$$(EI)_{eff} = E_a I_a + E_s I_s + K_e E_{cm} I_c \tag{11}$$

where E_a is the modulus of elasticity of the structural steel, E_s is the modulus of elasticity of reinforced steel, E_{cm} is the secant modulus of elasticity of concrete, and K_e is a correction factor that should be taken equal to 0.60 according to Eurocode 4 [24]. The modulus of elasticity of the concrete E_{cm} is reduced to the value $E_{c,eff}$ that is determined as:

$$(EI)_{eff} = E_{cm} \frac{1}{1+(N_{G,Ed}/N_{Ed})\varphi_t} \tag{12}$$

where φ_t is the creep coefficient according to § 5.4.2.2 Equation (2) of Eurocode 4 [24], N_{Ed} is the total design normal force, $N_{G,Ed}$ is the portion of N_{Ed} given by the permanent loads. Eurocode 4 [24] shows that for the determination of the internal forces the design value of effective flexural stiffness $(EI)_{eff,II}$ should be determined from the following expression:

$$(EI)_{eff,II} = K_0\left(E_a I_a + E_s I_s + K_{e,II} E_{cm} I_c\right) \tag{13}$$

where $K_{e,II}$ is a correction factor which should be taken as 0.50 and K_0 is a calibration factor which should be taken as 0.90.

3.5 Shear connectors

The shear studs are required along the horizontal steel beams and at the corners of the SRCWs. In fact, the absence of the shear connectors, especially between the steel beams HE and the RC infill wall, causes an important decrement both of the initial stiffness and of the strength of the hybrid wall [17] that must be avoided. The design of the shear studs can be performed according to rules suggested in § 6.6.4 and Annex C of Eurocode 2 [22]. The sizes of the steel studs should be designed in order to transmit shear forces, at floor level, between the frame of the SRCW and the RC infill wall. Shear studs might be possibly replaced by steel trusses in order to transmit the same amount of shear forces.

4 Case study

4.1 Geometry and loads

The considered case study is a four-storey building located at Domegge di Cadore (Italy), initially conceived without SRCWs (model SCC.1). Floor dimensions are 42.50 m × 12.80 m (Figure 7) and the inter-storey height is 3.40 m. Floors are made of unidirectional self-supporting slabs for lengths up to 5 m, partially precast and cast in situ. Permanent load G_k is of 4.30 kN/m^2 including structural (2.30 kN/m^2) and non-structural loads (2.00 kN/m^2). Variable actions Q_k are equal to 2.00 kN/m^2 in the residential areas and 4.00 kN/m^2 for areas subjected to crowd such as passages and stairs (Figure 7). The roof (Figure 8) has permanent load G_k of 4.00 kN/m^2 and includes both the structural (2.00 kN/m^2) and the non-structural load (2.00 kN/m^2). The variable actions Q_k is equal to 0.50 kN/m^2 except for the area highlighted in Figure 8 where Q is equal to 3.00 kN/m^2.

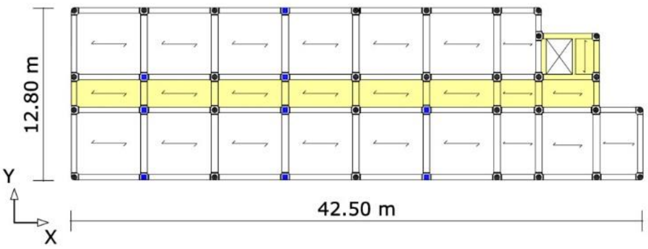

Figure 7 Floor geometry of SCC.1 without SRCWs. Filled area highlights the variable action, equal to 4 kN/m^2, concerning crowd. The concrete-filled composite columns have circular (black colour) and square (blue colour) sections.

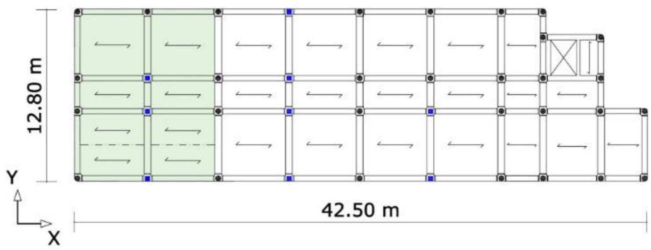

Figure 8 Roof geometry of SCC.1 without SRCWs. Filled area highlights the variable action equal to 3 kN/m^2.

For the considered site, according to the Italian building code [21], the reference peak ground acceleration a_g is equal to 0.133g; the soil factor (type C) and the topographic factors are equal to 1.5 and to 1.2, respectively (seismic spectra parameters given in Table 1).

Table 1 Acceleration response spectra parameters.

Parameter	Ultimate limit state (ULS)	Damage limit state (DLS)
a_g/g	0.133	0.051
F_0	2.488	2.483
T_C^* [s]	0.351	0.260
S_S	1.500	1.500
C_C	1.483	1.637
S_T [s]	1.200	1.200
S	1.800	1.800
T_B [s]	0.174	0.142
T_C [s]	0.521	0.426
T_D [s]	2.132	1.803

4.2 Structural solutions and seismic design

Four different structural solutions are considered in this study (Tables 2 and 3). The first solution (SCC.1) is made by MR frames made by concrete-filled composite columns and composite truss beams. No SRCWs are included. Columns have circular or square sections (Figure 7). The circular section columns have an external diameter equal to 508 mm and a steel thickness equal to 6.35 mm (Figure 7). The square cross section of some columns have dimensions of 400 mm × 400 mm and steel thickness equal to 12.5 mm. Circular and square section columns are made of steel S235 and steel S275, respectively; concrete C28/35 is used for all the considered concrete-filled hollow section columns. Composite truss beams are made of concrete C28/35, steel S355 and longitudinal reinforcing bars B450C. SCC.1 is designed considering a behaviour factor equal to 3.2 (Figure 9).

Table 2 Considered steel-concrete composite structures. External diameter (De) and thickness (t) of the steel section for the circular section columns; side (B) and thickness (t) of the steel section for the square section columns; use of shear hybrid walls (SRCW).

Model	Concrete-filled hollow section columns				SRCW
	Circular section		Square section		
	De (mm)	t (mm)	B (mm)	t (mm)	
SCC.1	508	6.35	400	12.50	no
SCC.2	508	6.35	400	12.50	yes
SCC.3	406	10.00	400	12.50	yes
SCC.4	406	10.00	350	12.00	yes

Table 3 SRCW system connected to the steel-concrete composite structures.

Model	SRCW system				
	square column		steel beam	RC infill wall	
	B (mm)	t (mm)		L (mm)	w (mm)
SCC.1	-	-	-	-	-
SCC.2	400	12.50	HE220B	2200÷2650	220
SCC.3	400	12.50	HE220B	2200÷2650	220
SCC.4	400	12.50	HE220B	1700	220

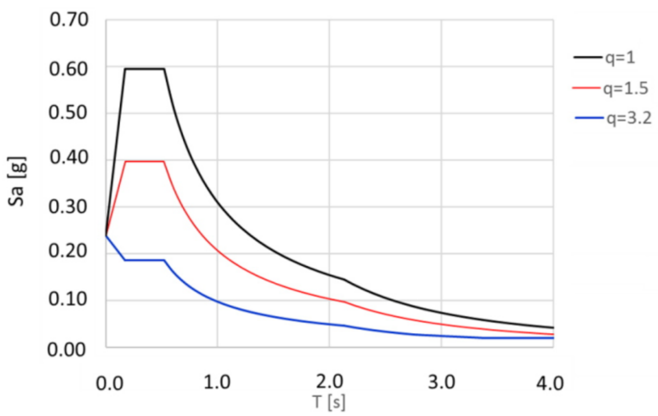

Figure 9 Elastic Acceleration response spectra (black colour) and design response spectra with behaviour factor q equal to 1.5 (red colour) and to 3.2 (blue colour) respectively.

The second structural solution (SCC.2) is made of the same steel-concrete composite structure of the case SCC.1 with the addition of six SRCW systems (Table 2) for each direction (Figure 10). Furthermore, composite truss beams are introduced near each SRCW such that the loads of the floors do not rest directly on the SRCWs that aim at supporting the horizontal forces.

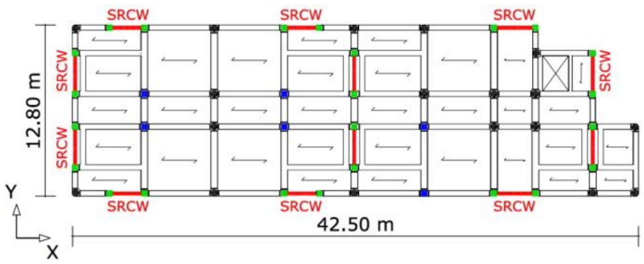

Figure 10 Floor geometry of SCC.2 and SCC.3 with SRCWs.

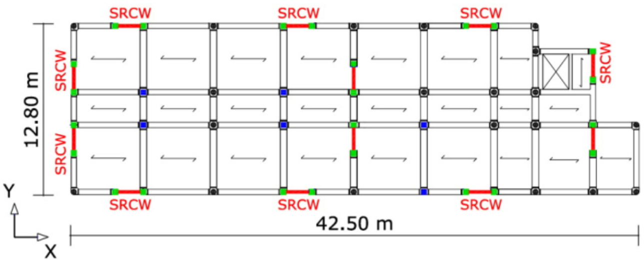

Figure 11 Floor geometry of SCC.4 with SRCWs.

The third (SCC.3) and fourth (SCC.4) structural solutions represent two levels of optimization of SCC.2. The case SCC.3 has the same structure of the case SCC.2, but the columns of the frames have different cross sections (Table 2). The case SCC.4 has cross sections of the composite columns (Table 2) and the length of the SRCWs (Table 3) reduced with respect to the previous cases. Furthermore, in this case the loads transmitted by the floors rest directly on the SRCW. The additional composite beam near each SRCW is removed in this case (Figure 11).

The SRCWs in SCC.2, SCC.3, and SCC.4, which represent the main horizontal resisting system, are conceived to remain elastic under the design seismic forces; thus, the behaviour factor is assumed equal to 1.5, as previously discussed. It is important to highlight that only the case SCC.1 was designed as a dissipative seismic structure with behaviour factor larger than 1.5. The increment of the seismic input (Figure 9), due to the reduction of the behaviour factor, is supported by the introduction of the SRCWs.

4.3 Numerical models

Finite elements models of the considered structures were implemented into the software SAP2000 Ultimate V20 through the use of frame elements. As an example Figure 12 shows a three-dimensional view of the model for SCC.3.

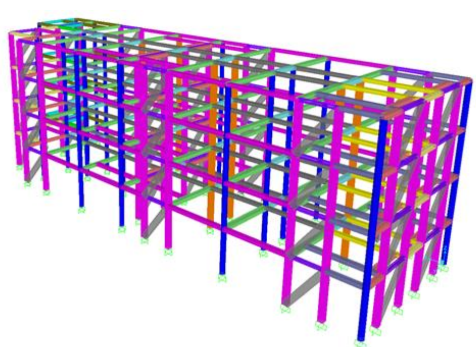

Figure 12 Three-dimensional view of the finite element model for SCC.3.

The stiffness of the steel-concrete composite columns was calculated according to § 7.7.2 of Eurocode 8 [2]. The effective modulus of elasticity for the concrete $E_{c,eff}$ was considered equal to the half of the modulus of elasticity of the concrete E_{cm} in order to take in account the creep effects as suggested by § 5.4.2.2 of Eurocode 4 [22]. The diagonal struts of the SRCWs were modelled as RC element, with section dimensions equal to 0.22 m × 0.51 m, pinned at their ends. Rigid floor constraints were implemented at each level.

4.4 Comparisons of the modal properties

Modal analysis provides useful information regarding the different stiffness of the cases investigated. The four structural models have the first and second vibration modes characterized by translations along the two horizontal (X and Y) directions; the third mode is characterized by torsional rotation (Z axis). The increment of the stiffness of the structure, due to the presence of the SRCWs, determined an important decrement of the vibration periods of the models for SCC.2, SCC.3, and SCC.4 (Table 4) compared to the model of SCC.1 where the SRCWs are not included.

Table 4 Vibration periods of the considered structural systems.

Vibration mode	Vibration period T (s)			
	SCC.1	SCC.2	SCC.3	SCC.4
1	0.692	0.358	0.360	0.410
2	0.678	0.323	0.325	0.393
3	0.588	0.262	0.263	0.323

The decrement of the fundamental vibration periods caused an important increment of the spectral acceleration value; this effect is further increased by the reduction of the behaviour factor q for the Ultimate Limit State (ULS) as shown in Figure 13.

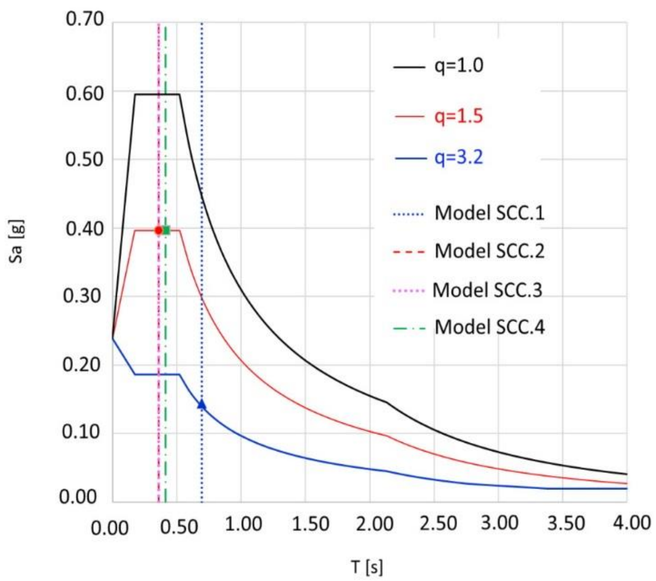

Figure 13 Acceleration response spectra (ULS) and the vibration periods (Table 4) of the considered structural systems.

4.5 Comparisons of SCC.2 to SCC.1 through modal response spectrum analysis

In order to understand the differences in the expected seismic performances between the case SCC.1 (steel-concrete MR frame without SRCWs designed as dissipative structure with q = 3.2) and the cases SCC.2, SCC.3, and SCC.4 (steel-concrete MR frame with SRCWs designed as elastic structures with q = 1.5), preliminary analyses were performed through the modal response spectrum approach, as contemplated in Eurocode 8 [2].

The comparison between the cases SCC.1 and SCC.2 shows that, despite of the increment of the spectral acceleration, the introduction of the SRCWs causes a decrease of the bending moments in the columns of the composite MR frames. The comparisons of the maximum bending moments and axial forces are reported in Table 5 for the perimeter circular columns, in Table 6 for the internal circular columns, and in Table 7 for the internal square columns. It is remarked that the reductions of the bending moments in the columns are significant considering the different behaviour factors q considered (3.2 and to 1.5, respectively).

Table 5 Envelope of the axial forces and bending moments of the perimetral circular columns for SCC.1 and SCC.2.

Axial force or bending moment	SCC.1	SCC.2	$\Delta_{SCC.1}$ (%)
N_{min} (kN)	-843.72	-852.73	1.07
N_{max} (kN)	-194.49	376.17	-
$M_{y,max}$ (kNm)	137.38	117.82	-14.24
$M_{x,max}$ (kNm)	169.71	124.43	-26.68

Table 6 Envelope of the axial forces and bending moments of the internal circular columns for SCC.1 and SCC.2.

Axial force or bending moment	SCC.1	SCC.2	$\Delta_{SCC.1}$ (%)
N_{min} (kN)	-1056.22	-1060.82	0.44
N_{max} (kN)	-398.49	-402.20	0.93
$M_{y,max}$ (kNm)	137.12	116.13	-15.31
$M_{x,max}$ (kNm)	167.66	122.1	-27.17

Table 7 Envelope of the axial forces and bending moments of the internal square columns for SCC.1 and SCC.2.

Axial force or bending moment	SCC.1	SCC.2	$\Delta_{SCC.1}$ (%)
N_{min} (kN)	-1072.61	-1085.77	1.23
N_{max} (kN)	-498.87	-541.63	8.57
$M_{y,max}$ (kNm)	144.89	123.76	-14.58
$M_{x,max}$ (kNm)	196.21	110.16	-43.86

Differences between the compression axial forces of the internal columns are generally negligible (as shown in Tables 6 and 7). A detailed analysis of the results shows that only three circular columns at the building perimeter experience tensile axial forces in some seismic combinations due to their proximity to the SRCWs. In fact, the steel-concrete composite columns of the SRCWs are affected by relevant axial forces due to the assumed structural scheme for the hybrid shear walls (Figure 5). On the other hand, the internal columns are affected by only compression axial forces (Tables 6 and 7) despite of the increment of the seismic accelerations due to the decrement of the behaviour factor q.

The compression and tension axial forces of the columns of the SRCWs are significant (Table 8) as expected considering the adopted structural scheme (Figure 5), as already observed in

[3], [16] despite the reduction of the seismic action due to the considered dissipative seismic behaviour, as previously commented in this same section.

Table 8 Envelope of the axial forces and bending moments of the square columns of the SRCWs of the SCC.2.

Axial force or bending moment	SCC.2
N_{min} (kN)	-1865.93
N_{max} (kN)	2076.79
$M_{y,max}$ (kNm)	129.81
$M_{x,max}$ (kNm)	139.69

This comparison shows that the introduction of the SRCWs allows a significant reduction of the inter-storey drifts (Tables 9 and 10), thus, accomplishing the initial goal to adopt SRCWs designed in the elastic range to limit structural and non-structural damage. In fact, the presence of SRCWs allows reducing the inter-storey drifts despite of the increment of the seismic acceleration for the Damage Limitation Limit State (DLS) as shown in Figure 14.

Table 9 Inter-storey drifts (X-direction) of SCC.1 and SCC.2.

Level (m)	SCC.1	SCC.2	$\Delta_{SCC.1}$ (%)
3.4	0.0044	0.0020	-54.5
6.8	0.0069	0.0030	-56.5
10.2	0.0057	0.0032	-43.9
13.6	0.0036	0.0027	-25.0

Table 10 Inter-storey drifts (Y-direction) of SCC.1 and SCC.2.

Level (m)	SCC.1	SCC.2	$\Delta_{SCC.1}$ (%)
3.4	0.0056	0.0020	-64.9
6.8	0.0089	0.0030	-66.1
10.2	0.0074	0.0029	-61.2
13.6	0.0047	0.0024	-48.4

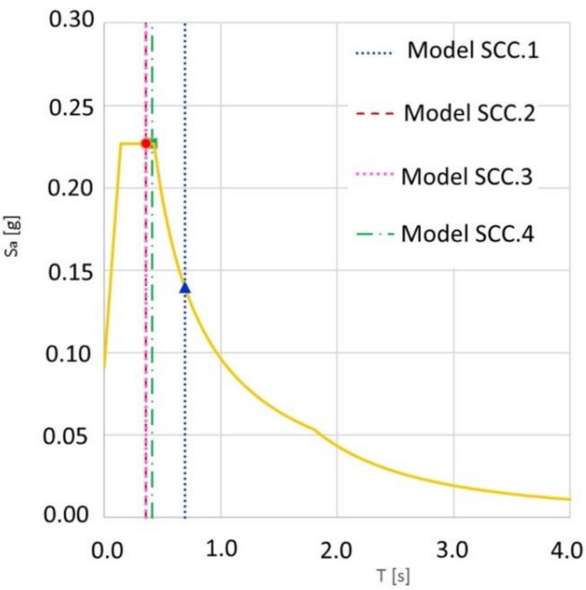

Figure 14 Design spectra (DLS): accelerations and vibration periods (Table 4) of the considered structural systems.

4.6 Comparisons of SCC.3 to SCC.1 and SCC.2 through modal response spectrum analysis

The decrease of the bending moments in the concrete-filled composite columns, due to SRCWs, allowed the reduction of the cross section for the circular columns (Table 1) in the SCC.3. As already observed, the vibration periods for SCC.3 are smaller than those of SCC.1 (Table 4) and very close to those of SCC.2 (Figure 13). The internal columns of SCC.3 highlighted a larger reduction (compared to the reduction achieved in SCC.2) of the bending moments (Table 11 and Table 12) with respect the bending moments of the columns of SCC.1. The decrease of the cross section for the circular columns of SCC.3 does not influence both to the axial forces and the bending moments of the SRCWs (Table 13). In addition, the differences between the compression forces of diagonal struts of the SRCWs for SCC.2 and SCC.3 are negligible (Table 14). Furthermore, the inter-storey drifts of SCC.3 are very close to those of SCC.2.

Table 11 Envelope of the axial forces and bending moments of the internal circular columns for SCC.1 and SCC.3.

Axial force or bending moment	SCC.1	SCC.3	$\Delta_{SCC.1}$ (%)
N_{min} (kN)	-1056.22	-1030.85	-2.40
N_{max} (kN)	-398.49	-397.48	-0.25
$M_{y,max}$ (kNm)	137.12	77.62	-43.39
$M_{x,max}$ (kNm)	167.66	83.34	-50.29

Table 12 Envelope of the axial forces and bending moments of the internal square columns for SCC.1 and SCC.3.

Axial force or bending moment	SCC.1	SCC.3	$\Delta_{SCC.1}$ (%)
N_{min} (kN)	-1072.61	-1086.79	1.32
N_{max} (kN)	-498.87	-541.07	8.46
$M_{y,max}$ (kNm)	144.89	125.23	-13.57
$M_{x,max}$ (kNm)	196.21	111.67	-43.09

Table 13 Envelope of the axial forces and bending moments for the square columns of the SRCWs.

Axial force or bending moment	SCC.2	SCC.3	$\Delta_{SCC.2}$ (%)
N_{min} (kN)	-1865.93	-1873.67	0.41
N_{max} (kN)	2076.79	2088.4	0.56
$M_{y,max}$ (kNm)	129.81	131.19	1.06
$M_{x,max}$ (kNm)	139.69	140.06	0.26

Table 14 Envelope of the axial forces (kN) for the diagonal struts of the SRCWs.

Diagonal struts	SCC.2	SCC.3	$\Delta_{SCC.2}$ (%)
C40-C2	-1120.26	-1133.48	1.18
C4-C41	-1093.07	-1108.95	1.45
C7-C8	-1210.00	-1227.66	1.46
C47-C33	-1135.52	-1148.21	1.12
C35-C48	-1110.17	-1125.50	1.38
C38-C39	-1213.00	-1228.82	1.30

4.7 Comparison of SCC.4 to SCC.1, SCC.2 and SCC.3 through modal response spectrum analysis

Finally, the additional optimization of SCC.4 is considered. This configuration has cross sections of the composite columns (Table 2) and the length of the SRCWs (Table 3) that are smaller than those of the previous cases. Furthermore, as already illustrated, the loads transmitted by the floors and the roof are supported by the hybrid shear walls; in fact, there are not additional composite truss beams near each SRCW. The hybrid shear walls cause a decrement of the vibrational period (Table 4). This reduction is smaller than those of SCC.2 and SCC.3 due to the different stiffness of the SRCWs (Table 4 and Figure 13). Once again, the reduction of the bending moments of the internal columns (Tables 15 and 16) highlights the effectiveness of the SRCWs in supporting the seismic actions, despite the smaller dimensions considered in this fourth case. The internal steel-concrete composite columns are not affected by tensile axial forces under design seismic actions.

Table 15 Envelope of the axial forces and bending moments of the internal circular columns for SCC.1 and SCC.4.

Axial force or bending moment	SCC.1	SCC.4	$\Delta_{SCC.1}$ (%)
N_{min} (kN)	-1056.22	-1029.25	-2.55
N_{max} (kN)	-398.49	-368.51	-7.52
$M_{y,max}$ (kNm)	137.12	97.81	-28.67
$M_{x,max}$ (kNm)	167.66	113.88	-32.08

Table 16 Envelope of the axial forces and bending moments of the internal square columns for SCC.1 and SCC.4.

Axial force or bending moment	SCC.1	SCC.4	$\Delta_{SCC.1}$ (%)
N_{min} (kN)	-1072.61	-1042.17	-2.84
N_{max} (kN)	-498.87	-490.72	-1.63
$M_{y,max}$ (kNm)	144.89	105.13	-27.44
$M_{x,max}$ (kNm)	196.21	104.22	-46.88

The differences between SCC.1 and SCC.4 in terms of the bending moments, due to seismic loads, for composite truss beams along the X direction (Figure 15) and composite truss beams along the Y direction (Figure 16) are generally small (Tables 17 and 18, respectively), with more evident decrements in the Y direction when SCC.4 is considered instead of SCC.1. For the Y direction the differences between the bending moments of SCC.1 and SCC.2 (Table 19) are bigger than those of the previous comparison (Table 18) due to the different sizes of the SRCWs. This result highlighted the importance of the choice of the stiffness in the design of the SRCWs.

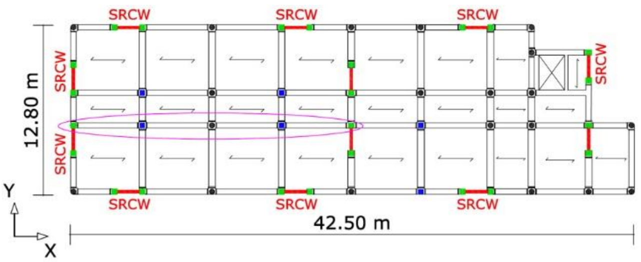

Figure 15 Composite truss beams (X direction) investigated to compare SCC.1 and SCC.4 (Table 17).

Table 17 Envelope of the bending moments (kNm) due to seismic actions of considered composite truss beams for SCC.1 and SCC.4 (X direction).

Model	Beam 11-12	Beam 12-13	Beam 13-14	Beam 14-15
	$M_{r-e}^{(-)}$	$M_{r-e}^{(-)}$	$M_{r-e}^{(-)}$	$M_{r-e}^{(-)}$
SCC.1	-67.49	-62.69	-64.07	-62.77
SCC.4	-64.51	-59.43	-60.82	-64.23
$\Delta_{SCC.1}$ (%)	-4.42	-5.20	-5.07	2.33

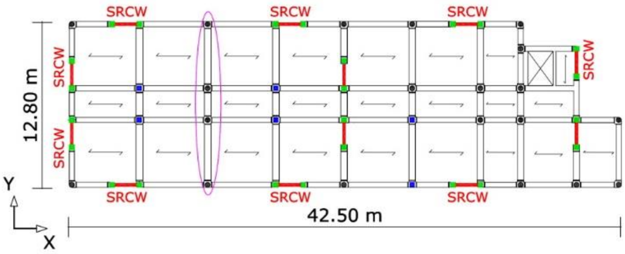

Figure 16 Composite truss beams (Y direction) investigated to compare SCC.1 and SCC.4 (Table 18).

Table 18 Envelope of the bending moments (kNm) due to seismic actions of considered composite truss beams for SCC.1 and SCC.4 (Y direction).

Model	Beam 3-13	Beam 13-23	Beam 23-34
	$M_{r-e}^{(-)}$	$M_{r-e}^{(-)}$	$M_{r-e}^{(-)}$
SCC.1	-143.37	-127.51	-146.19
SCC.4	-129.78	-108.27	-132.05
$\Delta_{SCC.1}$ (%)	-9.48	-15.09	-9.67

Table 19 Envelope of the bending moments due to seismic actions of the considered composite truss beams for SCC.1 and SCC.2 (Y direction).

Model	Beam 3-13	Beam 13-23	Beam 23-34
	$M_{r-e}^{(-)}$	$M_{r-e}^{(-)}$	$M_{r-e}^{(-)}$
SCC.1	-143.37	-127.51	-146.19
SCC.2	-117.00	-92.90	-118.10
$\Delta_{SCC.1}$ (%)	-18.39	-27.14	-19.21

SRCWs allow reducing the differences between the bending moments due to seismic actions at ULS and those caused by only gravitational loads, as for example shown in Table 20 where SCC.1, SCC.3, and SCC.4 are compared. Given that SRCWs in SCC.3 are stiffer than those in SCC.4, the effect of reducing the seismic contribution in the bending moment is more pronounced for SCC.3.

Table 20 Envelope of bending moments (kNm) due to gravitational loads (M_{r-g}) and seismic actions (M_{r-e}) of composite truss beams SCC.1, SCC.3, and SCC.4 (Y direction).

Model	Beam 3-13			Beam 23-34		
	$M_{r-g}^{(-)}$	$M_{r-e}^{(-)}$	Δ_g (%)	$M_{r-g}^{(-)}$	$M_{r-e}^{(-)}$	Δ_g (%)
SCC.1	-107.37	-143.37	33.53	-103.78	-146.19	40.87
SCC.3	-107.37	-110.46	2.88	-103.78	-110.64	6.61
SCC.4	-107.37	-129.78	20.87	-103.78	-132.05	27.24

SRCWs allow reducing the base shear forces for the internal columns (Table 21). The reduction of the cross section sizes of the columns of the structure connected to the SRCWs, such as for the SCC.3, caused an additional reduction.

Table 21 Total base shear forces of the internal columns.

	SCC.1	SCC.2	SCC.3	SCC.4
Base shear force (kN)	594.62	530.2	453.45	477.16
$\Delta_{SCC.1}$ (%)	-	-10.83	-23.74	-19.75

These results demonstrate that the increment of the seismic actions for the cases with SRCWs, due to the reduction of the behaviour factor q, is counterbalanced by the SRCWs themselves. The considered SRCWs support more than the 80% of the total base shear force due to the design seismic input, as reported in Table 22.

Table 22 Shares (%) of the total base shear force for the columns and the hybrid shear walls of the considered structural configurations.

SCC.2		SCC.3		SCC.4	
Columns	SRCWs	Columns	SRCWs	Columns	SRCWs
16.52 %	83.48%	13.61 %	86.39 %	17.08 %	82.92 %

5 Conclusion

In this study the use of hybrid steel and concrete walls as seismic-resistant systems was explored with the objective of limiting damages to structural and non-structural components in steel-concrete moment resisting frames. The considered hybrid system is constituted by a one-bay steel frame with reinforced concrete infill walls at each floor level. The nodes of the steel frame are shaped to foster the development of a concrete strut in the infill wall, working as a diagonal brace for the steel frame. The hybrid wall system is conceived to remain in the elastic range, thus, a non-dissipative behaviour is assumed in the seismic design, not requiring capacity design procedures.

Different designs options for a case study building were analysed. The starting structural solution was a moment-resisting steel-concrete composite frame with no hybrid walls, designed with dissipative behaviour as allowed by European building codes. Afterwards, the proposed hybrid walls were added to the moment-resisting steel-concrete composite frame and the design assumption switched from dissipative to non-dissipative seismic behaviour. The hybrid walls allow bearing the increment of the seismic actions due to the reduction of the behaviour factor (from 3.2 of the dissipative moment-resisting frame to 1.5 of the non-dissipative moment-resisting frame with hybrid walls).

Numerical results showed that the use of hybrid shear walls allows to significant reduce: (1) interstorey drifts; (2) bending moments in the columns of the moment-resisting frames; (3) bending moments due to seismic actions in the beams of the moment-resisting frames. It is remarked that these results were obtained regardless the increment in the seismic action due to reduction of the behaviour factor. Furthermore, the SRCWs allow reducing the base shear forces of the columns of the moment-resisting frames connected to the hybrid shear walls. This evidence allowed to reduce the cross sections of the moment-resisting frames connected to the hybrid walls.

Additional optimization of the steel-concrete composite frames and of the components of the hybrid walls could be obtained by considering the dissipation capacity of the system (behaviour factor larger than 1.50). Thus, further studies based on nonlinear analyses and experimental tests should be foreseen to set the basis for more advanced design rules.

Acknowledgements

This research is supported by Tecnostrutture s.r.l., Italy, in a joint research project at the University of Camerino, Italy, and the University College of London, United Kingdom. The support is gratefully acknowledged.

References

[1] Paulay, T.; Priestley, M.J.N. (1992) *Seismic Design of Reinforced Concrete and Masonry Buildings*, Wiley, New York.

[2] EN 1998-1 (2004) *Eurocode 8. Design of structures for earthquake resistance - Part 1: General rules, seismic actions and rules for buildings.*

[3] Dall'Asta, A.; Leoni, G.; Zona, A.; Hoffmeister, B.; Bigelow, H.; Degée, H.; Braham, C.; Bogdan, T.; Salvatore, W.; Morelli, F.; Tsintzos, P.; Karamanos, S. A.; Varelis, G. E.; Galazzi, A.; Medici, E.; Boni, P. (2015) *Innovative hybrid and composite steel-concrete structural solutions for building in seismic area*, Final Report, EUR 26932 EN, European Commission.

[4] El-Tawil, S.; Harries K.; Fortney, P.; Shahrooz, B.; Kurama, Y. (2010) *Seismic design of hybrid coupled wall systems: State of the art*, Journal of Structural Engineering **136**, 755–769.

[5] Zona, A.; Degeé, H.; Leoni, G.; Dall'Asta, A. (2016) *Ductile design of innovative steel and concrete hybrid coupled walls*, Journal of Constructional Steel Research, **117**, 204-213.

[6] Zona, A.; Tassotti, L.; Leoni, G.; Dall'Asta, A. (2018) *Nonlinear seismic response analysis of an innovative steel-and-concrete hybrid coupled wall system*, Journal of Structural Engineering, **144**, 7, 04018082.

[7] Das, R.; Zona, A.; Vandoren, B.; Degeé, H. (2018) *Optimizing the coupling ratio in the seismic design of HCW systems with shear dissipative links*, Journal of Constructional Steel Research, **147**, 393-407.

[8] Das, R.; Steensels, R.; Dragan, D.; Vandoren, B.; Degée, H. (2020) *Characterization and optimization of a steel beam to RC wall connection for use in innovative hybrid coupled wall systems*, Structures, **23**, 111–125.

[9] Shahrooz, B. M.; Fortney, P. J.; Harries, K. A. (2018) *Steel coupling beams with a replaceable fuse*, Journal of Structural Engineering, **144**, 04017210.

[10] Plumier, A.; Dragan, D.; Quang Huy, N.; Degée, H. (2017) *An Analytical Design Method for Steel-Concrete Hybrid Walls*, Structures, **9**, 185–199.

[11] Hu, H.; Nie, J.; Fan, J.; Tao, M.; Wang, Y.; Li, S. (2016) *Seismic behavior of CFST-enhanced steel plate-reinforced concrete shear walls* , Journal of Constructional Steel Research, **119**, 176–189.

[12] Suizi, J.; Wanlin, C.; Zibin, L.; Wei, D.; Yingnan, S. (2019) *Experimental Study on a Prefabricated Lightweight Concrete-Filled Steel Tubular Framework Composite Slab Structure Subjected to Reversed Cyclic Loading*, Applied Sciences, **9**, 6, 1264.

[13] Wang, W.; Song, J.; Hou, M.; Liu, G.; Wang, W. (2019) *Experimental study and numerical simulation of replaceable corrugated steel plate-concrete composite shear walls*, Soil Dynamics and

Earthquake Engineering, **127**, 105827.

[14] Ghazizadeh, S.; Cruz-Noguez, C. A.; Li, Y. (2019) *Numerical study of hybrid GFRP-steel reinforced concrete shear walls and SFRC walls*, Engineering Structures, **180**, 700–712.

[15] Petkune, N.; Donchev, T.; Hadavinia, H.; Wertheim, D.; Limbachiya, M. (2018) *Comparison of the behaviour of steel, pure FRP and hybrid shear walls under cyclic seismic loading in aspect of stiffness degradation and energy absorption*, Construction and Building Materials, **165**, 621–630.

[16] Dall'Asta, A.; Leoni, G.; Morelli, F.; Salvatore, W.; Zona, A. (2017) *An innovative seismic-resistant steel frame with reinforced concrete infill walls*, Engineering Structures, **141**, 144-158.

[17] Morelli, F.; Mussini, N.; Salvatore, W. (2019) *Influence of shear studs distribution on the mechanical behaviour of dissipative hybrid steel frames with r.c. infill walls*, Bulletin of Earthquake Engineering, **17**, 2, 957-983.

[18] Piattoni, Q.; Zona, A.; Freddi, F.; Leoni, G.; Dall'Asta, A.; Argentoni, A. (2019) *Preliminary studies on a prefabricated hybrid steel-concrete seismic-resistant wall*, Proceedings of XVIII ANIDIS Congress – 15th-19th September, Ascoli Piceno, **SS11**, 29-38.

[19] Scozzese, F.; Terracciano, G.; Zona, A.; Della Corte, G.; Dall'Asta, A.; Landolfo, R. (2018) *Analysis of seismic non-structural damage in single-storey industrial steel buildings*, Soil Dynamics and Earthquake Engineering, **114**, 505-519.

[20] Scozzese, F.; Terracciano, G.; Zona, A.; Della Corte, G.; Dall'Asta, A.; Landolfo, R. (2018) *Modelling and seismic response analysis of Italian code-conforming single-storey steel buildings*, Journal of Earthquake Engineering, 22, 168-197.

[21] Italian building code (2018) *Norme tecniche per le costruzioni*, D.M. 17/01/2018, in Italian.

[22] EN 1992-1-1 (2005) *Eurocode 2. Design of concrete structures - Part 1-1: General rules and rules for buildings.*

[23] EN 1993-1-1 (2005) *Eurocode 3. Design of steel structures - Part 1-1: General rules and rules for buildings.*

[24] EN 1994–1 (2006) *Eurocode 4. Design of composite steel and concrete structures - Part 2: General rules and rules for bridges.*